



# Phases in antiferroelectric-side Rb<sub>1-x</sub>(ND<sub>4</sub>)<sub>x</sub>D<sub>2</sub>AsO<sub>4</sub> crystals studied by complex permittivity

Authors: C.-S. Tu and V.H. Schmidt

NOTICE: this is the author's version of a work that was accepted for publication in *Ferroelectrics*. Changes resulting from the publishing process, such as peer review, editing, corrections, structural formatting, and other quality control mechanisms may not be reflected in this document. Changes may have been made to this work since it was submitted for publication. A definitive version was subsequently published in [Ferroelectrics](#), [VOL# 227, (1999)] DOI# [10.1080/00150199908224197](https://doi.org/10.1080/00150199908224197)

C.-S. Tu and V.H. Schmidt, "Phases in antiferroelectric-side Rb<sub>1-x</sub>(ND<sub>4</sub>)<sub>x</sub>D<sub>2</sub>AsO<sub>4</sub> crystals studied by complex permittivity," *Ferroelectrics* 227, 141-151 (1999).  
<http://dx.doi.org/10.1080/00150199908224197>

Made available through Montana State University's [ScholarWorks](#)  
[scholarworks.montana.edu](http://scholarworks.montana.edu)

# PHASES IN ANTIFERROELECTRIC-SIDE $\text{Rb}_{1-x}(\text{ND}_4)_x\text{D}_2\text{AsO}_4$ CRYSTALS STUDIED BY COMPLEX PERMITTIVITY\*

CHI-SHUN TU<sup>a,†</sup> and V. HUGO SCHMIDT<sup>b</sup>

<sup>a</sup> *Department of Physics, Fu-Jen University, Taipei, Taiwan 242, Republic of China;*

<sup>b</sup> *Department of Physics, Montana State University, Bozeman, Montana 59717*

*(Received 19 September 1998)*

Temperature and frequency dependent dielectric measurements in the mixed ferroelectric (FE)–antiferroelectric (AFE) system  $\text{Rb}_{1-x}(\text{ND}_4)_x\text{D}_2\text{AsO}_4$  (DRADA- $x$ ) (for ammonium concentrations  $x = 0.39, 0.55$  and  $0.69$ ) are reported for measured fields along the  $a$  axis. These measurements, together with our previous light scattering results, confirm the phase coexistence of paraelectric (PE) and antiferroelectric (AFE) phases in both  $x = 0.55$  and  $0.69$  crystals. Phase coexistence of deuteron-glass (DG) and antiferroelectric orderings is evidenced by the weak frequency dispersions (which occur below  $\sim 100$  K) in both dielectric permittivities ( $\epsilon'_a$  and  $\epsilon''_a$ ) for the  $x = 0.39$  crystal. The temperature-dependent data  $\epsilon''_a(f, T)$  prove the existence of an electric dipolar relaxation process below  $\sim 100$  K. The activation energy and attempt frequency corresponding to this relaxation process are calculated.

*Keywords:* Mixed FE-AFE system; dielectric permittivity; antiferroelectric

## I. INTRODUCTION

In the mixed FE-AFE system  $A_{1-x}(\text{ND}_4)_x\text{D}_2\text{BO}_4$  [ $A = \text{Rb}$  (or  $\text{K}$ ,  $\text{Cs}$ ) and  $B = \text{As}$  (or  $\text{P}$ )], there is competition between FE and AFE orderings, each characterized by specific configurations of the acid deuterons.<sup>[1–13]</sup> The random distribution of the  $\text{Rb}^+$  and  $\text{ND}_4^+$  ions is the main source of frustration which can increase local structural competition such that the

---

\* This work is dedicated in honor of Professor Lev Shuvalov on the occasion of his 75th birthday, recognizing his many contributions to knowledge of hydrogen-bonded and other ferroelectrics, and his service for three decades on the Editorial Board of *Ferroelectrics*.

<sup>†</sup>Corresponding author.

long-range electric order disappears. Instead of a typical sharp FE or AFE phase transition, phase coexistence (such as PE/FE and PE/AFE) becomes a characteristic of such mixed compounds. As an example, in  $\text{Rb}_{0.9}(\text{ND}_4)_{0.1}\text{D}_2\text{AsO}_4$  freezing-in of the  $\text{ND}_4$  reorientations and associated  $\text{O}-\text{D}\cdots\text{O}$  “acid” deuteron bond rearrangement is responsible for FE/PE phase coexistence as evidenced by gradual changes with temperature seen in dielectric, NMR and light scattering results.<sup>[8–13]</sup>

In deuteron glass the randomness depends on the  $\text{Rb}^+$  and  $\text{ND}_4^+$  cation placement. In ferroelectric  $\text{RbD}_2\text{AsO}_4$  (DRDA) if one looks down along the  $c$  axis, the deuterons in  $\text{O}-\text{D}\cdots\text{O}$  bonds lying along the  $a$  (or  $b$ ) axis are near the tops of  $\text{AsO}_4$  groups for one type of FE domain. In antiferroelectric  $\text{ND}_4\text{D}_2\text{AsO}_4$  (DADA) two adjacent  $\text{N}-\text{D}\cdots\text{O}$  bonds (viewed along the  $c$  axis) of a given  $\text{ND}_4^+$  ion are short and the other two adjacent  $\text{N}-\text{D}\cdots\text{O}$  bonds are long. In this arrangement a given  $\text{O}-\text{D}\cdots\text{O}$  bond shares oxygens with one short and one long  $\text{N}-\text{D}\cdots\text{O}$  bond, with  $\text{O}-\text{D}$  near the long bond and  $\text{D}\cdots\text{O}$  near the short bond. In a mixed crystal, these inconsistent ordering schemes favored by the arsenate and ammonium ions cause frustration and prevent either ferroelectric or antiferroelectric phases.

The phase diagram obtained for  $\text{Rb}_{1-x}(\text{NH}_4)_x\text{H}_2\text{AsO}_4$  (RADA) on the basis of dielectric measurements is asymmetric when compared to that of RADP. The glass state of RADA occurs for an ammonium concentration  $0.13 \leq x \leq 0.49$ .<sup>[6,7]</sup> In recent years, some measurements in the DRADA- $x$  system have been made on ferroelectric-side crystals such as  $x=0, 0.10$  and  $0.28$ .<sup>[8–12]</sup> However, only few experiments were done on antiferroelectric-side compounds ( $x \geq 0.35$ ).<sup>[2,3,6]</sup> Complete understanding of this mixed system is still lacking. This motivated us to carry out temperature-dependent dielectric measurements on DRADA- ( $x = 0.39, 0.55$  and  $0.69$ ). These results will be discussed with the earlier temperature-dependent results of Brillouin and Raman light scattering.

## II. EXPERIMENTAL PROCEDURE

Single crystals of  $\text{Rb}_{1-x}(\text{ND}_4)_x\text{D}_2\text{AsO}_4$  ( $x = 0.39, 0.55$  and  $0.69$ ) were grown from aqueous solutions with certain ratios of  $\text{RbD}_2\text{AsO}_4$  (DRDA) and  $\text{ND}_4\text{D}_2\text{AsO}_4$  (DADA) by slow evaporation of  $\text{D}_2\text{O}$  in an atmosphere of argon gas. The  $\text{ND}_4$  concentrations were determined from the ratio of Rb and N atoms by X-ray photoelectron spectroscopy (XPS). The relation of  $\text{ND}_4$  concentration between  $x'$  (in solution) and  $x$  (in crystal) is linear within experimental error ( $\pm 3\%$ ) and is shown in Figure 1. The samples to be

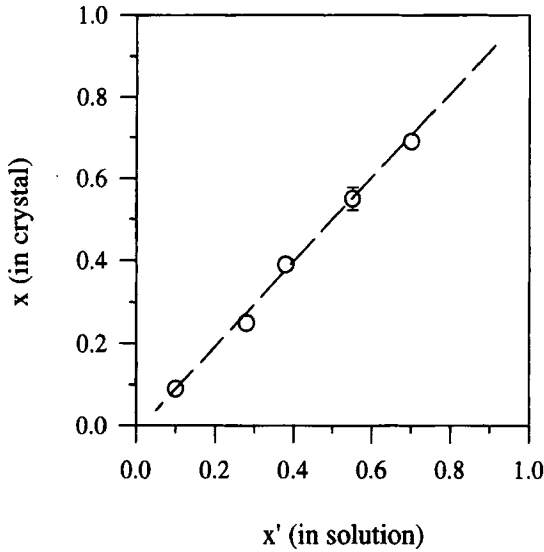


FIGURE 1 The relation of  $\text{ND}_4$  concentration between  $x'$  (in solution) and  $x$  (in crystal).

studied were cut out of the crystals along the  $a$  axis. Their surfaces were polished and coated with silver paste electrodes. A Wayne-Kerr Precision Analyzer Model PMA3260A with four-lead connections and a Janis CCS-150 closed cycle refrigerator were used with a LakeShore Model 340 temperature controller from 20 to 300 K.

### III. RESULTS AND DISCUSSION

Figure 2 shows the temperature dependences of the real part of the dielectric permittivity  $\epsilon'_a$  for various values of ammonium concentration  $x = 0.69$ ,  $0.55$  and  $0.39$ . The figure presents data taken at 300 kHz. Compared with the pure antiferroelectric crystal  $\text{ND}_4\text{D}_2\text{AsO}_4$  (DADA), these three mixed crystals show a gradual transition which begins at  $T_m = 240$ ,  $186$  and  $140$  K for  $x = 0.69$ ,  $0.55$  and  $0.39$ , respectively. Here  $T_m$  corresponds to the temperature giving maximum value of the dielectric permittivity  $\epsilon'_a$ . These facts suggest that these crystals do not have an abrupt antiferroelectric transition. Instead, the random rubidium and ammonium ion placements cause local variations in the strength of the antiferroelectric ordering tendency, giving a gradual increase in such ordering and corresponding decrease in permittivity as temperature decreases and the ammonium and

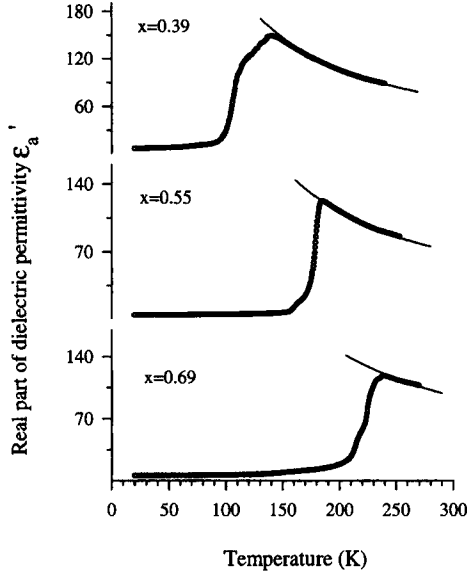


FIGURE 2 Temperature dependences of the real part of the dielectric permittivity  $\epsilon'_a$  for DRADA- $x = 0.69, 0.55$  and  $0.39$ , taken at the frequency of the measuring electric field  $f = 300$  kHz. The solid lines are the Curie–Weiss fits with parameters given in Table I.

acid hydrogen bond rearrangements freeze out. The dielectric constant  $\epsilon'_a$  from slightly above  $T_m$  up towards higher temperatures is found to obey the Curie–Weiss behavior. The solid lines in Figure 2 represent fits to the Curie–Weiss formula: <sup>[14]</sup>

$$\epsilon'_a = \frac{C}{T - T_w}, \quad (1)$$

where  $C$  is the Curie–Weiss constant and  $T_w$  is the Curie–Weiss temperature. Table I shows these fitting parameters for various concentrations  $x$ .

What are the origins of the temperature-dependent dielectric phenomenon shown in Figure 2 for DRADA-0.69? Its permittivity exhibits a gradual

TABLE I Parameters from the fits of Eq. (1) to temperature-dependent dielectric permittivity  $\epsilon'_a$  measured at  $f = 300$  kHz for various ammonium concentrations  $x$

$x$	$C(K)$	$T_w(K)$	$T_m(K)$
0.69	27500	11	240
0.55	18800	31	186
0.39	19700	18	140

transition which begins to drop rapidly at  $T_m \sim 240$  K, but then an additional rather weak shoulder was observed at  $\sim 215$  K. Such a transition cannot be described by a typical phenomenological theory applied for pure FE or AFE transitions.<sup>[14]</sup> The real part of dielectric permittivity  $\epsilon'_a$  deviates from the Curie–Weiss law below  $\sim 240$  K. However, there is no frequency dispersion observed in either  $\epsilon'_a$  or  $\epsilon''_a$  for DRADA-0.69 within the measured temperature range. In our earlier results, the acoustic-phonon frequency exhibits successive slope changes at  $\sim 230$  and  $\sim 160$  K as temperature decreases.<sup>[13]</sup> The acoustic damping also has an abrupt drop and reaches a minimum near 160 K.<sup>[13]</sup> Furthermore, in the low-temperature region, the Raman spectra of DRADA-0.69 show almost the same pattern as pure  $\text{ND}_4\text{D}_2\text{AsO}_4$  (DADA), that has an AFE phase below  $\sim 300$  K.<sup>[13]</sup> Thus, one can conclude that DRADA-0.69 possesses nearly complete AFE ordering below  $T \sim 160$  K. What is the situation between  $\sim 240$  K and  $\sim 160$  K? Comparison can be made to earlier dielectric results from the ferroelectric-side DRADA- $x$  system, in which a similar dielectric maximum anomaly was observed in DRADA-0.10.<sup>[8, 9]</sup> It was connected to PE/FE phase coexistence due to the freezing-in of  $\text{ND}_4$  reorientations associated with local destruction of FE ordering in DRADA-0.10. For DRADA-0.69, one can expect that the partial replacement of  $\text{ND}_4$  molecular groups by Rb atoms can cause growth of local structural competition (between FE and AFE orderings), so that long-range AFE ordering could be partially suppressed. In other words, neither a pure AFE nor PE phase but rather a PE/AFE phase coexistence will develop. Thus, the broad dielectric maximum, located at  $T_m \sim 240$  K in DRADA-0.69, can be linked to the onset of phase coexistence of the PE/AFE type. We conclude that PE/AFE phase coexistence begins at  $T_m \sim 240$  K and below  $T \sim 160$  K the AFE ordering becomes completely dominant in the  $x = 0.69$  crystal. The lack of dispersion in the observed frequency range, up to  $f_m = 300$  kHz, requires that the dielectric time constant range in the PE phase does not extend up beyond  $(2\pi f_m)^{-1} = 0.53$  microseconds. This conclusion only applies above 160 K, the temperature range in which PE phase material exists. The origin of the shoulder at 215 K and the tail extending down to 160 K is not understood. Either the AFE transition has this strange temperature dependence, or there is some intermediate, possibly incommensurate, phase.

Compared to  $x = 0.69$ ,  $x = 0.55$  displays a more abrupt transition for which  $\epsilon'_a$  begins to drop at  $T_m \sim 185$  K and an additional weak cusp was also observed at  $\sim 165$  K. The dielectric constant  $\epsilon'_a$  falls to 6 below  $T_m$ . This is smaller than the value of  $\epsilon'_a$  for the pure ( $x = 0$ ) sample below  $T_c$ , thus ruling out the possibility of observing a glass transition below 165 K.

However, there is no frequency dispersion observed in either permittivity,  $\epsilon'_a$  or  $\epsilon''_a$ , for  $x = 0.55$ . In our previous results, the  $A_1$ ,  $B_2$  and  $E$  symmetries of  $x = 0.55$  all have the same Raman spectra as those of pure DADA in the low-temperature region.<sup>[13]</sup> The temperature dependence of the acoustic phonon frequency also exhibits successive anomalies (two slight plunges) at  $\sim 180$  and  $\sim 110$  K. In addition, the acoustic damping displays an abrupt drop and reaches a minimum near 110 K.<sup>[13]</sup> Based on the above discussion, it is clear that the  $x = 0.55$  crystal has complete AFE ordering below  $T \sim 110$  K. In a similar way as in DRADA-0.69, the broad dielectric maximum located at  $T_m \sim 185$  K can be connected to the onset of formation of PE/AFE phase coexistence. Below  $T \sim 110$  K, the crystal has complete AFE ordering. Whatever disorder may exist between 110 K and 150 K has no effect on the permittivity, which remains essentially flat up to 150 K.

For  $x = 0.39$ , precise measurement at temperatures below 100 K proved the existence of frequency dispersion in both the real and imaginary parts of the dielectric permittivity  $\epsilon'_a(f, T)$  and  $\epsilon''_a(T, f)$ , which are illustrated in Figures 3 and 4. The  $\epsilon''_a(T, f)$  vs.  $T$  curve (Fig. 4) shows scatter which may be due to the weak values of  $\epsilon''_a$  that are over two orders of magnitude smaller than those found for DRADA-0.28, within the concentration range in which only the deuteron glass (DG) phase can occur.<sup>[1]</sup> These dispersion phenomena observed in both  $\epsilon'_a$  and  $\epsilon''_a$  confirm that the deuteron-glass state begins to be evidenced in this frequency range below  $T \sim 100$  K in  $x = 0.39$ . This DG phase material coexists with a much larger fraction of the dominant AFE phase, from 100 K down to 20 K where evidence for the DG phase disappears.

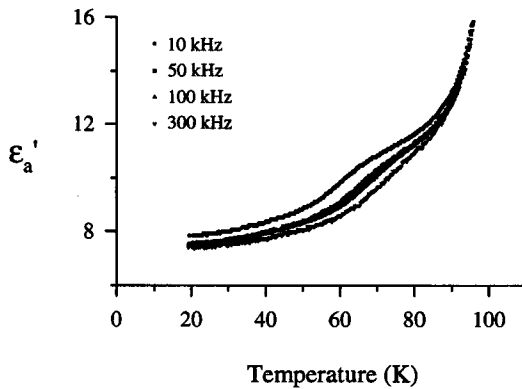


FIGURE 3 Frequency dispersion of the real part of the dielectric permittivity  $\epsilon'_a(f, T)$  for DRADA- $x = 0.39$ .

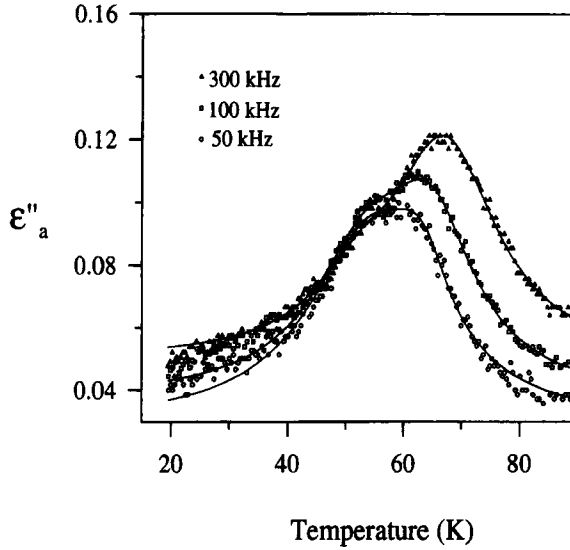


FIGURE 4 Frequency dispersion of  $\varepsilon''_a(f, T)$  for DRADA- $x = 0.39$ . The solid lines are the fits of Eq. (2).

The composite shape of the temperature dependences of  $\varepsilon''_a$  implies that two kinds of electric dipolar mechanisms could be involved. To check this, the experimental results were fitted to two Lorentzian functions (which fits better than two Gaussian functions);

$$\varepsilon''_a(T) = A \left[ 1 + \frac{(T - T_{gI})^2}{\Delta_I^2} \right]^{-1} + B \left[ 1 + \frac{(T - T_{gII})^2}{\Delta_{II}^2} \right]^{-1}, \quad (2)$$

where  $T_{gI}$  and  $T_{gII}$  are temperatures corresponding to the peaks in  $\varepsilon''_a$ . Figure 5 illustrates the best fits for frequency 300 kHz. It was found that the relaxation occurring in the higher temperature region (60–80 K) obeys the exponential Vogel–Fulcher equation, that has been used to describe the relaxation process in proton (and deuteron) glass:<sup>[4–6]</sup>

$$f = f_o e^{\frac{-E_a}{k(T_g - T_o)}}, \quad (3)$$

where  $f$  is the measured frequency,  $f_o$  is the attempt frequency, and  $E_a$  is the activation energy for orientation of electric dipoles.  $T_o$  is the Vogel–Fulcher

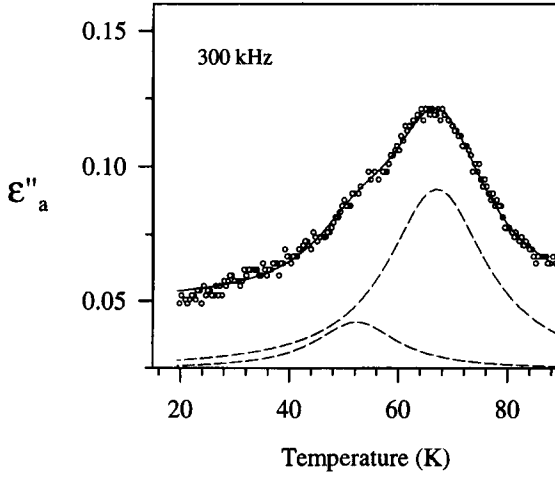


FIGURE 5 The fits of Eq. (2) to the experimental data  $\varepsilon''_a(f, T)$  measured at frequency 300 kHz. The contribution of two different mechanisms is marked by dashed curves.

temperature and  $T_g$  is the temperature where  $\varepsilon''_a$  reaches its maximum value. Our results for the activation energy attempt frequency, and the Vogel–Fulcher temperature for DRADA-0.39 are:  $E_a \sim 57$  meV (663 K),  $f_o \sim 3 \times 10^{12}$  Hz, and  $T_o \sim 26$  K. This activation energy is smaller than that for DRADA-0.10 by almost a factor of 2 and is almost the same as for the undeuterated  $\text{Rb}_{0.9}(\text{NH}_4)_{0.1}\text{H}_2\text{AsO}_4$  (RADA-0.1).<sup>[12]</sup> Here,  $2E_a$  is approximately the energy required to create a  $\text{DAsO}_4$ – $\text{D}_3\text{AsO}_4$  pair from two  $\text{D}_2\text{AsO}_4$  groups. However, the other maximum in  $\varepsilon''_a$  occurring in the lower temperature region (40–60 K) obeys neither the Vogel–Fulcher nor Arrhenius equations. It indicates that the system of electric dipole has another non-relaxation mechanism in the low-temperature region.<sup>[13]</sup> In our earlier Raman results, the  $A_1$  symmetry spectra of DRADA-0.39 shows a different spectrum compared with the  $A_1$  spectra of the pure AFE crystal DADA in the low-temperature region.<sup>[13]</sup> In addition, DRADA-0.39 has Raman spectra of the  $E$  and  $B_2$  configurations similar to those of DADA. These characteristics of the  $A_1$  and  $B_2$  (or  $E$ ) spectra of DRADA-0.39 imply that two distinct local structural phases exist in the low-temperature region, and one of them is associated with AFE ordering.<sup>[13]</sup> From the above considerations, we conclude that the break (at  $T \sim 100$  K) in  $\varepsilon'_a(f, T)$  (Fig. 3) indicates the onset of DG/AFE phase coexistence.

We can compare these results with others in the same range of  $x$ . First, for  $x = 0.28$  there is no indication of an AFE or FE transition, but only a

gradual onset of DG behavior, with an  $\varepsilon_a''$  peak of 29 at 300 Hz and 55 K. <sup>[1]</sup> For  $x = 0.39$ , exactly the same  $x$  value as one of our crystals, the results are qualitatively similar to ours. <sup>[2]</sup> Their  $T_m$  is 134 K whereas ours is 140 K. Their peak goes immediately into a fast drop below  $T_m$ , like our result for  $x = 0.55$  but unlike our  $x = 0.39$  curve which has a gentle slope between  $T_m$  and the fast drop range. Their dispersion behavior is quite similar to ours, including the appearance of two peaks in  $\varepsilon_a''$  which they fit with Gaussian functions. The fits to the two relaxation processes disagree, however. They can fit their low-temperature (30–50 K) relaxation to the Vogel–Fulcher law and their high-temperature (60–90 K) relaxation to the Arrhenius law, whereas our low-temperature (40–60 K) results fit neither law and our high-temperature (60–80 K) results fit the Vogel–Fulcher law.

For  $x = 0.46$  there is behavior qualitatively similar <sup>[3]</sup> to our observations for  $x = 0.39$  and 0.55. First,  $T_m$  is 162 K, which fits well with the values 140 K and 186 K we found for  $x = 0.39$  and  $x = 0.55$  respectively. Second, there is a double-humped dispersion as we observed for  $x = 0.39$ , which they fit with two Gaussians. In contrast to the shoulder in  $\varepsilon_a'$  we observed for  $x = 0.55$  (and 0.69), they found a linear gradual slope in the 60 to 150 K range below the temperature region of the fast drop.

These results strengthen the previous findings that there are two relaxation mechanisms for DRADA-0.39 and DRADA-0.46. <sup>[2, 3]</sup> One of these mechanisms, probably the one at higher temperature, most likely is the usual deuteron glass relaxation. The lower-temperature mechanism occurs in a temperature range in which over 99% of the crystal has antiferroelectric order, so it could result from deuteron rearrangement in antiferroelectric domain walls. Another possibility is switching of ferroelectric microdomains polarized along  $a$ . From Table I we see that the extrapolated temperature  $T_w$  for such a ferroelectric transition is in the 10 to 30 K range, and perhaps in a geometry confined by neighboring AFE domains it is higher. We note here that in the  $x = 0$  to  $x = 0.10$  region for DRADA and RADA,  $T_w$  for  $\varepsilon_a$  is negative but is becoming less negative with increasing  $x$ . <sup>[10]</sup> It would be of interest to measure permittivity along  $c$  for these crystals, because an  $a$ -axis ordering tendency would not contribute in this case, and for this higher  $x$  range there would be no domain wall contribution to  $\varepsilon_c$ .

The three frequency-independent features noted in measurements by us and others, <sup>[2, 3]</sup> namely the shoulders seen in some cases at temperatures below the steepest permittivity drop, and the gentler slopes seen in some cases on both sides of this drop, seem to be sample-dependent and we have no explanation for their origin.

## IV. CONCLUSIONS

From the temperature- and frequency-dependent dielectric spectra of DRADA-0.69, 0.55 and 0.39, successive phase transitions (PE ordering  $\rightarrow$  PE/AFE phase coexistence  $\rightarrow$  AFE ordering) are confirmed in both  $x = 0.55$  and  $0.69$ . There is no evidence for existence of deuteron-glass in  $x = 0.55$  and  $0.69$  samples for frequencies up to 300 kHz. Instead of PE/AFE coexistence,  $x = 0.39$  shows DG/AFE phase coexistence taking place below  $T \sim 100$  K. The temperature-dependent dielectric permittivity  $\epsilon''_a(f, T)$  proves the existence of an electric dipolar relaxation process forming among the antiferroelectric domains below  $\sim 100$  K. A similar dielectric behavior labeled "reentrant" by Takeshige *et al.* [15] in  $\text{Rb}_{0.25}(\text{NH}_4)_{0.75}\text{H}_2\text{PO}_4(\text{RADP}-0.75)$  is considered by us to also indicate the coexistence of proton-glass and antiferroelectric orderings. The maximum value of  $\epsilon'_a$  decreases with increasing  $x$ . The activation energy, the Vogel–Fulcher temperature and attempt frequency corresponding to this relaxation process are calculated. With the previous results for ferroelectric-side DRADA- $x$  systems ( $x = 0, 0.10$  and  $0.28$ ), we propose that the DG state should exist for the ammonium concentration range of  $0.2 \leq x < 0.39$ . The phase diagram of the DRADA- $x$  system is much more asymmetric as compared to that of  $\text{Rb}_{1-x}(\text{NH}_4)_x\text{H}_2\text{PO}_4(\text{RADP})$ . [5]

### *Acknowledgments*

The authors would like to express sincere thanks to Dan Brandt for crystal growth, and to F.-C. Zhov and C.-H. Yeh for help on experiments. This work was supported by NSC87-2112-M-030-001 and NSF Grant DMR-9520251.

### *References*

- [1] Schmidt, V. H., Trybula, Z., He, D., Drumheller, J. E., Stigers, C., Li, Z. and Howell, F. L. (1990). *Ferroelectrics*, **106**, 119.
- [2] Trybula, Z., Stankowski, J. and Los, S. (1993). *Physica B*, **191**, 312.
- [3] Trybula, Z., Waplak, S., Stankowski, J., Los, S., Schmidt, V. H. and Drumheller, J. E. (1994). *Ferroelectrics*, **156**, 371.
- [4] Courtens, E. (1984). *Phys. Rev. Lett.*, **52**, 69.
- [5] Courtens, E. (1987). *Ferroelectrics*, **72**, 229.
- [6] Trybula, Z., Stankowski, J., Szczepanska, L., Blinc, R., Weiss, A. and Dalal, N. S. (1988). *Physica B*, **153**, 143.
- [7] Kim, S. and Kwun, S. (1990). *Phys. Rev. B*, **42**, 638.
- [8] Tu, C.-S. and Schmidt, V. H. (1994). *Phys. Rev. B*, **50**, 16167.
- [9] Pinto, N. J., *Ph.D. Thesis*, Montana State University, 1993.

- [10] Pinto, N. J., Howell, F. L. and Schmidt, V. H. (1993). *Phys. Rev. B*, **48**, 5983.
- [11] Tu, C.-S., Chien, R.-M. and Schmidt, V. H. (1997). *Phys. Rev. B*, **55**, 2920.
- [12] Howell, F. L., Pinto, N. J. and Schmidt, V. H. (1992). *Phys. Rev. B*, **46**, 13762.
- [13] Tu, C.-S., Gao, S.-S., Jaw, R.-J., Xue, Z.-Q., Hwa, L.-G. and Schmidt, V. H. (1998). *Phys. Rev. B*, **58**, 5440.
- [14] Lines, M. E. and Glass, A. M., *Principles and Applications of Ferroelectrics and Related Materials* (Oxford, London, 1977).
- [15] Takashige, M., Terauchi, H., Miura, Y. and Hoshino, S. (1985). *J. Phys. Soc. Jpn.*, **54**, 3250.